Metallophysics and Advanced Technologies
Металофіз. новітні технол.
Metallofiz. Noveishie Tekhnol.
2021, vol. 43, No. 11, pp. 1443–1454
https://doi.org/10.15407/mfint.43.11.1443
Reprints available directly from the publisher

METALLIC SURFACES AND FILMS

PACS numbers: 62.20.Qp, 68.55.Nq, 81.05.Je, 81.05.Mh, 81.15.Rs, 81.40.-z

Properties of AlB_{12}–Al Electric Spark Coatings on D1 Aluminium Alloy

A. P. Umanskyi, M. S. Storozhenko, V. E. Sheludko, V. B. Muratov, V. V. Kremenitsky[*], I. S. Martsenyuk, M. A. Vasilkovskaya, A. D. Kostenko, A. A. Vasiliev, A. E. Terentiev, and D. S. Kamenskykh[**]

I. M. Frantsevich Institute for Problems in Materials Science, N.A.S. of Ukraine,
3 Academician Krzhyzhanovsky Str.,
UA-03142 Kyiv, Ukraine
[*]*Technical Centre, N.A.S. of Ukraine,*
13 Pokrovs'ka Str.,
UA-04070 Kyiv, Ukraine
[**]*V. P. Kukhar Institute of Bioorganic Chemistry and Petrochemistry,*
N.A.S. of Ukraine,
1 Murmanska Str.,
UA-02094 Kyiv, Ukraine

The article deals with the study of the structure and properties of electric spark coatings of AlB_{12}–50 wt.% Al aluminium-matrix composite electrode material on D1 aluminium alloy. Fundamental possibility of such coatings obtaining is estimated by theoretical calculation of Palatnik's criterion (0.59). Thermal conductivity coefficient and heat capacity of the composite are calculated or determined from an experiment. Mass transfer kinetics at electric spark alloying (ESA) is studied. Considering a rather high values of the cathode mass gain, the coating applied in 6 mode (E = 2.52 J, τ = 700 μs, ALIER-52 setup) is selected for further research. The thickness (h = 380 μm), microhardness (H_μ = 1.86 GPa, PMT-3 tester, P = 0.05 N) and wear at dry friction (13.7 mg/(km·cm^2), MT-68 friction machine, the pin-on-disk scheme, V = 4 m/s, P = 0.2 MPa, friction path S = 3 km) are determined for the coating. Phase composition of the coating is studied with DRON-3M diffractometer

Corresponding author: Volodymyr Yevhenovych Sheludko
E-mail: dep65@ipms.kiev.ua

Citation: A. P. Umanskyi, M. S. Storozhenko, V. E. Sheludko, V. B. Muratov, V. V. Kremenitsky, I. S. Martsenyuk, M. A. Vasilkovskaya, A. D. Kostenko, A. A. Vasiliev, A. E. Terentiev, and D. S. Kamenskykh, Properties of AlB_{12}–Al Electric Spark Coatings on D1 Aluminium Alloy, *Metallofiz. Noveishie Tekhnol.*, **43**, No. 11: 1443–1454 (2021), DOI: 10.15407/mfint.43.11.1443.

and elemental X-ray spectrum analysis of the surface and cross-section is carried out using a JEOL JSM-6490 LV scanning electron microscope equipped with an energy-dispersive X-ray microanalysis and reflected electron diffraction system. The following phases namely Al, Al_2O_3, small quantity of B, B_2O_3, Fe_2O_3, $AlFeO_3$, AlB_2 and AlB_{10} are revealed by X-ray analysis in the coating. The Al content (reaching 89.92 wt.% in certain zones) is more than the other phases content. This affects the coating strength under dry friction condition. The absence of the AlB_{12} phase is noteworthy. It can be explained by thermo-oxidative destruction of aluminium dodecaboride under severe conditions of ESA.

Key words: AlB_{12}–Al, ESA, mass transfer kinetics, structure, phase composition, microhardness, wear.

Статтю присвячено дослідженню структури та властивостей електроіскрових покриттів з алюмоматричного композиційного матеріалу AlB_{12}–50% мас. Al на алюмінієвому стопі Д1. Оцінено теоретичну можливість одержання таких покриттів за допомогою теоретичного розрахунку критерію Палатніка (0,59). Коефіцієнт теплопровідності та теплоємність композиту розрахували чи визначили експериментально. Досліджено кінетику масопереносу під час електроіскрового леґування (ЕІЛ). Зваживши на достатньо високі значення приросту катоду, для подальшого дослідження обрано покриття, що нанесене на шостому режимі (E = 2,52 Дж, τ = 700 мкс) установки ALIER-52. Для нього визначено: товщину (h = 380 мкм), мікротвердість (H_μ = 1,86 ГПа, ПМТ-3, P = 0,05 Н) та знос за сухого тертя (13,7 мг/(км·см^2), машина тертя МТ-68, схема тертя штифт–диск, V = 4 м/с, P = 0,2 МПа, путь тертя S = 3 км). Фазовий склад покриття вивчено за допомогою дифрактометра ДРОН-3М, а елементний рентґеноспектральний аналіз поверхні та поперечного перерізу проведено на скануальному електронному мікроскопі JEOL JSM-6490 LV, обладнаному системою енергодисперсійного рентґенівського мікроаналізу та дифракції відбитих електронів. РФА в покритті виявлено Al, Al_2O_3, сліди B, B_2O_3, Fe_2O_3, $AlFeO_3$, AlB_2 та AlB_{10}. Кількість Al (на деяких ділянках вона досягає 89,92% мас.) перевищує кількість інших фаз, що впливає на стійкість покриття в умовах сухого тертя. Звертає на себе увагу відсутність фази AlB_{12}, що є наслідком термооксидаційної деструкції додекабориду алюмінію у жорстких умовах ЕІЛ.

Ключові слова: AlB_{12}–Al, кінетика масопереносу, структура, фазовий склад, мікротвердість, знос.

(Received May 5, 2021)

1. INTRODUCTION

Aluminium alloys are widely used in aircraft and ship building, rocket science, automotive industry, building, electrical and packaging industry, and other industries [1–5].

This is due to their properties such as good corrosion resistance, rel-

atively high strength at low density, high electric, and heat conductivity etc. [6, 7]. In addition, they work well at low temperatures, have the ability to damp vibrations and absorb energy, and easily processed by most of the known metal-working technologies. Also they are easily amenable to reuse—recycling [6].

At the same time, their low operating characteristics (low hardness and insufficient wear resistance) oppose the widening of the area of their utilization to produce, for example, frame parts, and various friction couples [8].

As shows possible to eliminate the defects by applying of coatings with the use of concentrated energy flows: surface strengthening with ion implantation, ion-plasma spraying, micro arc oxidation, plasma electrolytic oxidation, anodizing, laser processing, and electric spark alloying (ESA) [4, 9–16]. One could say that ESA is a quite efficient (in a number of parameters) technique enabling, in general, simply to apply the coatings (with various materials) on the details surfaces, in particular, aluminium alloys.

In ESA, an electrode material (anode) is transferred to a surface of a detail (cathode) to form a hardened layer with improved physical and mechanical properties. Various refractory compounds, namely carbides, nitrides, aluminides, silicides, and borides can be used as an anode material [17–19]. Among the latter, aluminium dodecaboride AlB_{12} is of interest. Its synthesis from Al and BN, developed at the Frantsevich Institute for Problems of Materials Science of N.A.S. of Ukraine is more rational and economically efficient than direct one from Al and B [20]. In addition, AlB_{12} has a low density (~2.52 g/cm^3) and the particularity of its crystalline structure (icosahedral boric frame) determines its high hardness (22–24 GPa), and refractoriness (2070°C) [21].

However, the low crack resistance of aluminium dodecaboride significantly limits the scope of its application [21]; therefore, it is advisable to use AlB_{12} in combination with plastic metal bonds. It is promising to use aluminium, which is characterized by high plasticity, low density (2.7 g/cm^3) and low melting point (660°C).

Earlier Al is found to wet AlB_{12} well, with the formation of contact angles ($\theta \approx 20$ deg) and the secondary phases in the interaction zone at the Al–AlB_{12} interface are absent [21]. In addition, aluminium has a resistivity of 2.7 μΩ·cm, which is 60% less than that of copper, thereby acting as a kind of additive increasing the conductivity of the AlB_{12}–Al composite (a resistivity of AlB_{12}—10^6 μΩ·cm), which is of great importance in ESA.

So, the aim of the work is to investigate the possibility of using the composite material 'aluminium dodecaboride AlB_{12}–Al' for ESA-coatings on the aluminium alloys to obtain, and also to study the properties of these coatings.

2. EXPERIMENTAL DETAILS

The AlB_{12} samples are prepared from the powder synthesized at the IPMS of N.A.S. of Ukraine according to the procedure described in [22, 23]. A porous AlB_{12} ceramic frame is obtained. Then it is soaked with an Al melt in vacuum (vacuum level $1.33 \cdot 10^{-4}$ Pa) at a temperature of ~1100°C. This made it possible to obtain the aluminium-matrix composite of AlB_{12}–50 wt.% Al in the form of a bar of 50×50×5 mm in size, from which the electrodes for ESA are cut by the electro-erosion method.

Figure 1 shows the microstructure of the electrode material AlB_{12}–50 wt.% Al, obtained with a JEOL JAMP9500F microanalyzer. The structure of the material consists of three phases: a metal matrix, AlB_{12} grains (the size of which varies in the range of 1–4 μm) uniformly distributed in it and Al_2O_3 particles (Fig. 1, inset).

The chemical composition of the main phases of the composite AlB_{12}–50 wt.% Al is determined by micro X-ray spectral analysis (Table 1). ESA of the samples of D1 aluminium alloy (GOST 4784-97) of 11.3 mm in a diameter is carried out on ALIER-52 installation (SCINTI, Chisinau, RM) at the modes indicated in Table 2. At the same time, on an electronic balance OHAUS Adventurer AR0640 with an accuracy of 10^{-4} g, the specific erosion of the anode (Δa), the specific gain in the cathode mass (Δk), determined for each minute of processing of 1 cm^2 of the sample surface, are measured. The total anode erosion ($\sum \Delta a$) and gain in the cathode mass ($\sum \Delta k$) are calculated, as well as the average mass transfer coefficient $K' = \sum \Delta k / \sum \Delta a$, determined during the alloying time $\tau = 10$ min/cm^2.

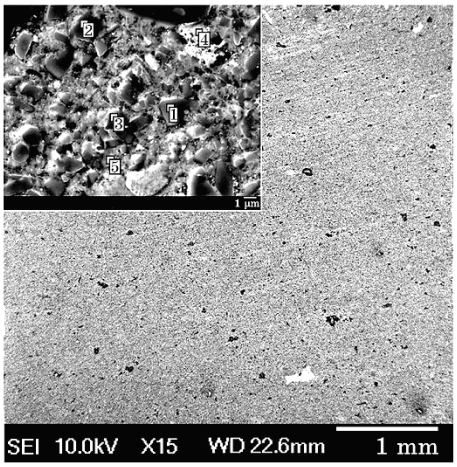

Fig. 1. Microstructure of the electrode material AlB_{12}–50 wt.% Al cross-section (inset—enlarged fragment with elemental analysis data).

TABLE 1. Chemical composition of the composite material AlB_{12}–50 wt.% Al (Fig. 1, inset).

Spectrum	Element, wt.%						Total
	B	C	N	O	Al	Fe	
1	82.07	0.66	–	0.03	16.92	0.32	100.00
2	81.52	0.88	0.15	0.05	17.00	0.40	100.00
3	78.77	3.94	1.01	0.45	15.83	–	100.00
4	0.26	0.60	0.67	47.02	51.45	–	100.00
5	1.37	1.97	0.11	1.81	94.74	–	100.00

TABLE 2. Technological parameters of ALIER-52 installation.

Mode	Pulse duration, $\mu s \pm 20\%$	Pulse current amplitude value, $A \pm 20\%$	Pulse energy, E, J
2	40	125	0.09
4	170	200	0.61
6	700	200	2.52

The density of the electrode material is determined by the method of hydrostatic weighing (GOST 25281-82). Its heat capacity is defined by calorimetric method (GOST 23250-78). Its thermal conductivity coefficient: according to the method described in [24]. Microhardness of the coatings is measured on a PMT-3 microhardness tester at a load of $P = 0.05$ N. Tribotechnical studies of the coatings are carried out on a MT-68 friction machine according to the pin-on-disk scheme in the mode: $P = 0.2$ MPa, $V = 4$ m/s, friction path $S = 3$ km. The hardened U8 steel (HRC 61-63) is used as a counterbody.

X-ray analysis of the coating surface is carried out on a DRON-3M diffractometer in CuK_α-filtered radiation. The structure of the coatings is studied using a JEOL JSM-6490 LV scanning electron microscope equipped with a Bruker Quantax CrystAling200 energy-dispersive X-ray microanalysis and reflected electron diffraction system.

3. RESULTS AND DISCUSSION

To estimate theoretically the interaction between an electrode and a substrate and, to some extent, predict a composition of a coating is possible using the Palatnik criterion [25, 26], which is related only to the physical constants of electrode materials as follows:

$$\frac{\tau_a}{\tau_k} \cong \frac{c_a \rho_a \lambda_a (T_a - T_0)^2}{c_k \rho_k \lambda_k (T_k - T_0)^2},$$

where τ_a and τ_k are the characteristic times of erosion (formation of melting centres in the discharge zone) of an anode and a cathode, respectively; c_a, c_k—heat capacity, J/(kg·K); ρ_a, ρ_k—density, kg/m^3; λ_a, λ_k—coefficient of thermal conductivity, W/(m·K); T_a, T_k—melting point, K; T_0 is the ambient temperature.

This ratio does not take into account a large number of factors affecting ESA process, but, it can be used for a quantitative evaluation of 3 types of interacting between an anode and a cathode made of various materials, namely:

– at $\tau_a << \tau_k$ a coating is formed on a cathode surface;

– at $\tau_a \sim \tau_k$ it is possible to form a coating as an alloy of an anode and a cathode;

– at $\tau_a >> \tau_k$ there is no transfer from an anode to a cathode, but a counter-transfer of material is possible [25, 26].

The data required for calculating the Palatnik criterion in our conditions are given in Table 3.

∗ Tm of the most low-melting phase (Al) is used for the calculation

It follows from the calculation that ES-coating on D1 substrate can be obtained with the material of AlB_{12}–50 wt.% Al.

Figure 2 shows the kinetic dependences of the total anode erosion and the cathode mass gain. These data indicate that at a pulse energy of E = 0.09 J (mode 2), for 4 min of alloying $\sum\Delta_k$ = 8.2 mg/cm^2 and $\sum\Delta_a$ = = 11 mg. By 9 min, $\sum\Delta_k$ and $\sum\Delta_a$ increase to 12.2 mg/cm^2 and 20.4 mg, respectively. The average coefficient of mass transfer K' at 4 min is 74.54%. The negative cathode mass gain is recorded for the first time at 10 min (*i.e.*, the threshold of the brittle destruction of the doped layer is T_x = 10). With an increase in the pulse energy to E = 0.61 J (mode 4), $\sum\Delta_k$ = 5.9 mg/cm^2, $\sum\Delta_a$ = 16.8 mg for 1 min of alloying. For 2 min these values are 22.5 mg/cm^2 and 68.8 mg, respectively. Under these conditions, K' is 35.11% for 1 min of treatment with a decrease to 32.7% at 2 min, T_x = 3.

Mode 6 (E = 2.52 J) is characterized by the values of $\sum\Delta_k$ = 120.2 mg/cm^2 (peak value) and $\sum\Delta_a$ = 371 mg for 3 min of treatment. K' = = 40.59% for 1 min followed by a decrease to 32.39% for 3 min T_x = 4.

Based on the fact that mode 6 is characterized by a rather high value

TABLE 3. Physical characteristics of the electrode materials and the value of the Palatnik criterion.

Characteristic	Anode (AlB_{12}–50 wt.% Al)	Cathode (D1) [27, 28]	The value of the Palatnik criterion τ_a/τ_c
λ, W/(m·K)	72.58	117	0.59
C_p, J/(kg·K)	918.88	922	
T_m, K	933*	923	
ρ, kg/m^3	2616	2800	

of ($\sum\Delta k$ (*i.e.* coating thickness) for 3 min of alloying, the coating applied in the mode is selected for further research.

Shown in Fig. 3 is the microstructure of the surface of ES-coating applied in mode 6. The surface consists of the aggregates containing (on average) 38 wt.% Al, 34 wt.% O, and 28 wt.% B.

X-ray analysis (Fig. 4) showed the presence of main phases of Al, Al_2O_3 and also small quantity of B, B_2O_3, Fe_2O_3, $AlFeO_3$, AlB_2, and AlB_{10}. Attention is drawn to two aspects.

Firstly, the absence of the AlB_{12} phase.

ESA process occurring at plasma temperatures ($2\cdot10^4$ K) in air is known to be accompanied by thermo-oxidative destruction of an anode and a cathode materials [29]. Such severe conditions aid in destructing of aluminium dodecaboride to constituent elements at $T = 2300$ K [30].

Secondly, the appearance of small quantity of $AlFeO_3$.

This compound (as only phase) is known to exist over the temperature range of 1318–1410°C (in a narrow concentration range near equimolar ratio of Al_2O_3/Fe_2O_3) and also in mix with solid solutions of

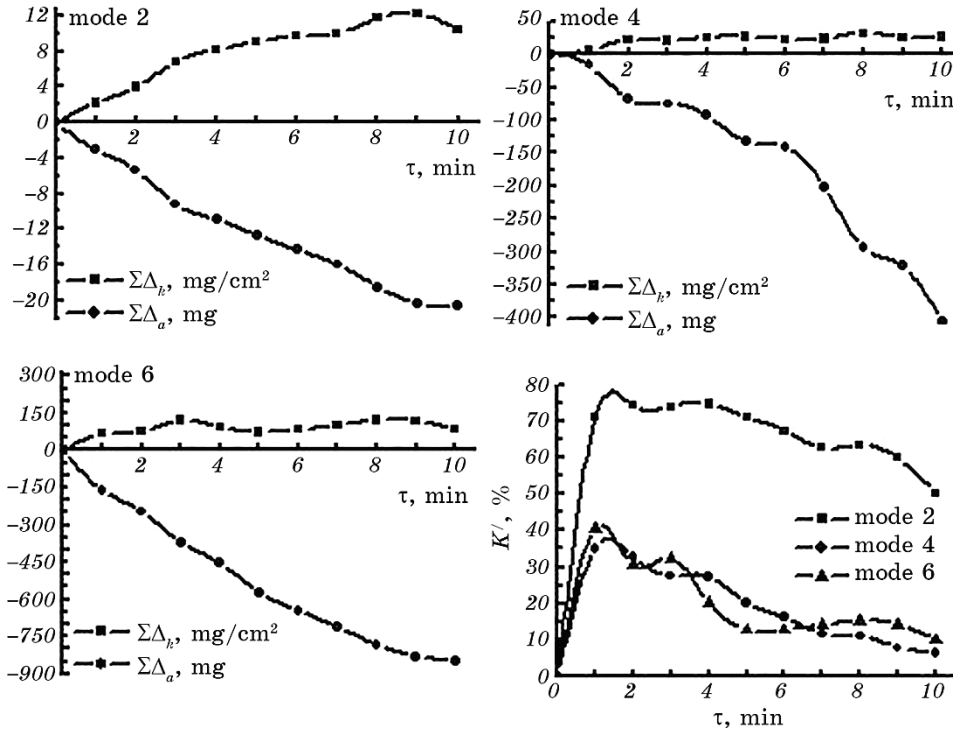

Fig. 2. Kinetic dependences of the total cathode mass gain $\sum\Delta_k$, the total anode erosion $\sum\Delta_a$, and the average value of the mass transfer coefficient K' at ESA of 1 cm² of D1 alloy.

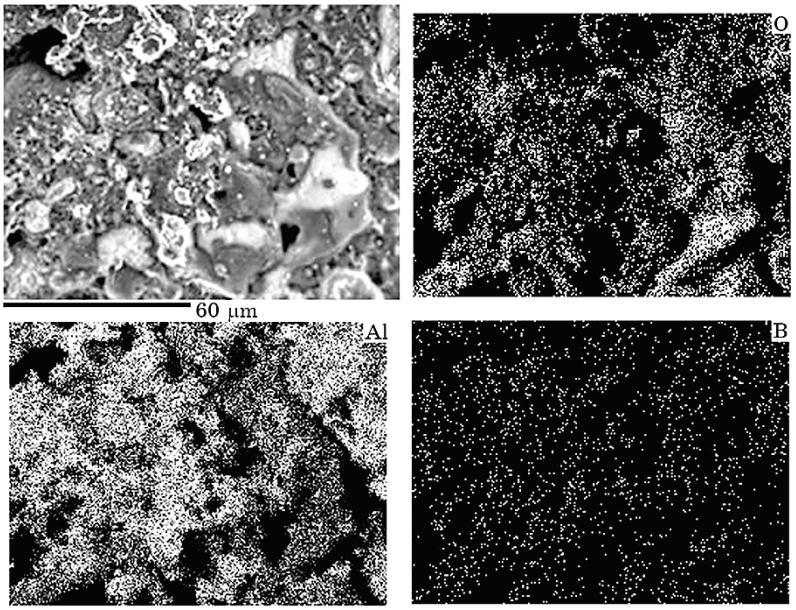

Fig. 3. Microstructure of ES-coating of AlB_{12}–50 wt.% Al on D1 alloy (mode 6) with distribution of the elements in X-ray radiation over its surface.)

corundum, hematite, and spinel [31].

It should also be noted that $AlFeO_3$ has sufficiently high hardness *HV* 1650–1700 [32].

In Figure 5 is shown the microstructure of the cross-section of ES-

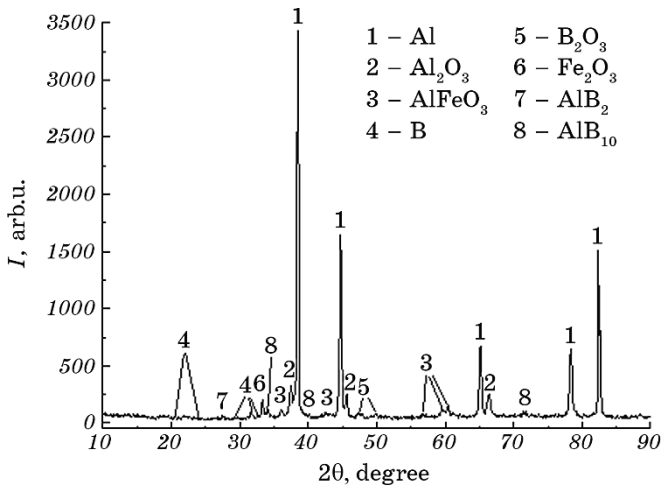

Fig. 4. Diffraction pattern of ES-coating of AlB_{12}–50 wt.% Al on D1 alloy.

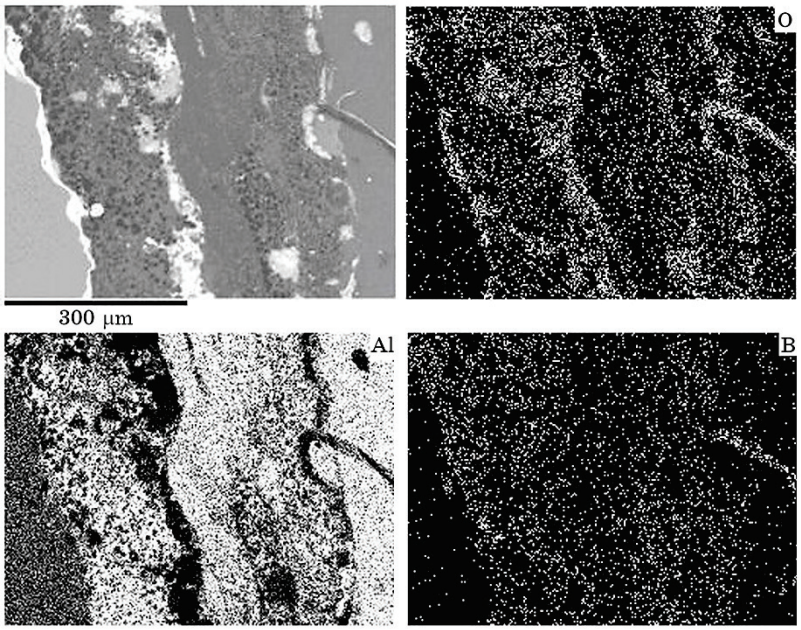

Fig. 5. Microstructure of the cross-section of ES-coating of AlB_{12}—50 wt.% Al on D1 alloy (mode 6) with distribution of the elements in X-ray radiation.

coating. These data indicate that Al, Al_2O_3, B_2O_3, and, perhaps, borates $Al_2O_3 \cdot B_2O_3$ are present in the coating layer [33, 34]. The thickness of the coating is ~380 μm, and its microhardness $H_\mu \sim 1.86$ GPa.

It is determined by tribological studies that the wear of the sample

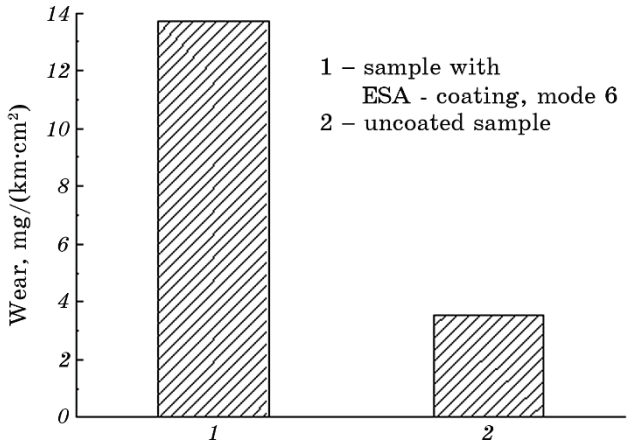

Fig. 6. Wear of ES-coating AlB_{12}–50 wt.% Al on D1 alloy.

with ES-coating is ~4 times greater than that of an uncoated one that may be concerned with a large amount of Al in the coating (Fig. 6). Though, according to X-ray analysis data, the coating contains phases (in small quantities) having significant hardness (Al_2O_3, $AlFeO_3$, AlB_2, and AlB_{10}), but, nevertheless, the main phase in the coating is Al. It is well known [35] that ESA-strengthening of Al-substrate by Al doesn't result in wear resistance increasing obviously owing to considerable brittleness of the applied coatings. It should also be noted that similar results are obtained for the ESA-coating applied on D1 alloy in mode 4 (the wear of the sample with ES-coating is also greater than that of an uncoated one).

4. CONCLUSION

1. The process of the formation of ES-coatings of the material AlB_{12}–50 wt.% Al on D1 aluminium alloy has been studied. Based on the analysis of the kinetic dependences of mass transfer, the optimal processing mode is determined—6 (E = 2.52 J). The one is characterized by a rather high value of the total cathode mass gain in the first minutes of alloying.
2. On mode 6, the coating having the thickness of ~380 μm and microhardness H_μ ~ 1.86 GPa is obtained. However, it has low wear resistance that can be explained by prevalent content of Al in the coating.
3. The system of AlB_{12}–Al is unfit to obtain wear-resistant coatings on aluminium alloys (duralumin type), a typical representative of which is D1 alloy.

REFERENCES

1. I. N. Fridlyander, *Tekhnologiya Lyogkih Splavov*, **4**: 12 (2002) (in Russian).
2. A. A. Mityaev, S. B. Belikov, and I. P. Volchok, *Vestnik Dvigatelestroeniya*, **1**: 155 (2006) (in Russian).
3. *Aluminum Alloys: Preparation, Properties and Application* (Ed. Erik L. Persson) (New York, NY, USA: Nova Science Publishers Inc.: 2011).
4. *ASM Specialty Handbook®. Aluminum and Aluminum Alloys* (Ed. by J. R. Davis&Associates) (Russell Township, Geauga County, OH, USA: ASM International: 1993).
5. V. A. Duyunova, A. A. Leonov, and S. V. Molodtsov, *Trudy VIAM*, **2**(86): 22 (2020) (in Russian).
6. R. Cobden, *Aluminum: Physical Properties, Characteristics and Alloys* (TALAT Lecture 1501: EAA: 1994).
7. *Aluminum Alloys: Their Physical and Mechanical Properties* (Eds. J. Hirsch, B. Skrotzki, and G. Gottstein) (Weinheim: Germany: Wiley-VCH Verlag GmbH & Co. KGaA: 2008), vol. 1.
8. V. D. Aleksandrov, *Poverhnostnoe Uprochnenie Alyuminievykh Splavov* [Surface Hardening of Aluminum Alloys] (Moscow: Tekhnopoligrafcentr: 2002)

(in Russian).
9. O. Yu. Usanova, A. V. Ryazantseva, I. L. Savelev, and V. S. Timohin, *J. Phys.: Conf. Ser.*, **1515**, No. 2: 022074 (2020).
10. V. I. Agafii, V. I. Petrenko, V. M. Fomichev, V. I. Yurchenko, E. V. Yurchenko, and A. I. Dikusar, *Surf. Eng. Appl. Elect.*, **49**, No.3: 181 (2013).
11. G. Renna, P. Leo, G. Casalino, and E. Cerri, *Adv. Mater. Sci. Eng.*, Article ID 8563054, 11 pages (2018).
12. Q. Zhu, B. Zhang, X. Zhao, and B. Wang, *Coatings*, **10**, Iss. 2: 128 (2020).
13. Ya. S. Kuzin, M. A. Fomina, I. A. Kozlov, and A. E. Kutyrev, *Trudy VIAM*, **4–5** (88): 70 (2020) (in Russian).
14. M. Ezzat, M. A. El-Waily, M. Abdel-Rahman, and Y. Ismail, *Surf. Rev. Lett.*, **25**, No. 4: 1850079 (2018).
15. W. Pakieła, L. A. Dobrzanski, K. Labisz, T. Tanski, K. Basa, and M. Roszak, *Arch. Metall. Mater.*, **61**, No. 3: 1343 (2016).
16. V. A. Duyunova, I. A. Kozlov, M. S. Oglodkov, and A. A. Kozlova, *Trudy VIAM*, **8** (80): 79 (2019) (in Russian).
17. A. D. Verkhoturov, I. A. Podchernyaeva, L. F. Pryadko, and F. F. Egorov, *Elektrodnye Materialy dlya Elektroiskrovogo Legirovaniya* [Electrode Materials for Electrospark Alloying] (Moscow: Nauka: 1988) (in Russian).
18. A. D. Verkhoturov and S. V. Nikolenko, *Uprochnyayushchie Tekhnologii i Pokrytiya*, No. 2: 13 (2010) (in Russian).
19. A. D. Verkhoturov, V. I. Ivanov, and L. A. Konevtsov, *Surf. Eng. Appl. Elect.*, **55**, No. 3: 241 (2019).
20. O. O. Vasiliev, V. B. Muratov, and T. I. Duda, *Physics and Chemistry of Solid State*, **18**, No. 3: 358 (2017).
21. P. S. Kisly, V. A. Neronov, T. A. Prikhna, and Yu. V. Bevza, *Boridy Aljuminiya* [Aluminum Borides] (Kiev: Naukova Dumka: 1990) (in Russian).
22. V. B. Muratov, P. V. Mazur, V. V. Garbuz, E. V. Kartuzov, and O. O. Vasiliev, *Sposib Oderzhannya Poroshku Dodekaborydu Alyuminiyu AlB_{12}* [The Method of Obtaining of AlB_{12} Aluminium Dodecaboride Powder]: Patent 107193 UA. MPK (2016.01), C01B 35/04, C01F 7/00 (Promyslova Vlasnist, No. 10: 4.52) (2016) (in Ukrainian).
23. P. V. Mazur, V. B. Muratov, V. V. Garbuz, E. V. Kartuzov, and O. O. Vasiliev, *Udarostijka Keramika na Osnovi Dodekaborydu Alyuminiyu* [Aluminium Dodecaboride-Based Crash-Proof Ceramics]: Patent 107259 UA. MPK (2016.01), C22C 1/04, C01B 35/00, B22F 3/04, C04B 111/20 (Promyslova Vlasnist, No. 10: 4.60) (2016) (in Ukrainian).
24. G. N. Dulnev and Yu. P. Zarichnyak, *Teploprovodnost Smeseyi Kompozitsionnykh Materialov* [Thermal Conductivity of Mixtures and Composite Materials] (Leningrad: Energiya: 1974) (in Russian).
25. L. S. Palatnik, *Dokl. Acad. Nauk SSSR, LXXXIX*, No. 3: 455 (1953) (in Russian).
26. O. S. Manakova, A. E. Kudryashov, and E. A. Levashov, *Surf. Eng. Appl. Elect.*, **51**, No. 5: 413 (2015).
27. metallicheckiy-portal.ru/marki_metallov/alu/D1
28. thermalinfo.ru
29. V. S. Kovalenko, A. D. Verkhoturov, L. F. Golovko, and I. A. Podchernyaeva, *Lazernoe i Electroerozionnoe Uprochnenie Materialov* [Laser and Electroerosion Hardening of Materials] (Moscow: Nauka: 1986) (in Russian).

30. T. Atoda, I. Higashi, and M. Kobayashi, *Sci. Pap. Inst. Phys. Chem. Res.*, **61**, No. 3: 92 (1967).
31. V. I. Mikhailov, Poluchenie i *Fiziko-Himicheskie Svoystva Materialov na Osnove Nanodispersnykh Oksidov Alyuminiya i Zheleza (III)* [Obtaining and Physical-Chemical Properties of Materials Based on Nanodispersed Oxides of Aluminum and Iron (III)] (Thesis of Disser. for Cand. Chem. Sci.) (Syktyvkar: Institute of Chemistry Komi Science Centre UB RAS: 2016) (in Russian).
32. L. V. Koroleva, *Recent Advances in Abrasives Research* (Ed. Ing. Dirk Bähre, PhD) (New York, NY, USA: Nova Science Publishers Inc.: 2013), p. 173.
33. S. Okada and T. Atoda, *J. Ceram. Association, Japan*, **88**, Iss. 1021: 547 (1980) (in Japanese).
34. G. Will, *Zeitschrift für Kristallogr.*, **128**: 156 (1969).
35. A. P. Abramchuk, G. A. Bovkun, V. V. Mikhailov, and Yu. G. Tkachenko, *Electronnaya Obrabotka Materialov*, **3**: 25 (1987) (in Russian).